



Corrosion Behavior of (Copper/Nickel) step-wise Functionally Graded Materials

Dheya Abdulamer ^{a,*} , Noor Sh Ghafil ^b , Dhuha Albusalih ^c , Alaa Abdulhasan Atiyah ^a

^a University of Technology- Iraq

^b Ministry of Education, Iraq

^c University of Al-Qadisiyah Iraq -AL-Diwaniyah

* Corresponding author: E-mail address: diaa.diaa197@gmail.com

Received 22.08.2024; accepted in revised form 29.11.2024; available online 17.03.2025

Abstract

The present paper involves studying of the corrosion behaviour of five layers Cu/Ni Functionally Graded Materials (FGMs) in a 3.5 % NaCl solution to examine corrosion potentials (E_{corr}), corrosion current densities (i_{corr}) and Tafel slope. Three series of FGMs samples, labeled A₁-A₆, B₁-B₆, and C₁-C₆ were prepared using different experimental conditions of compaction pressure (0.7, 1 and 1.3 MPa), sintering temperature (650, 750 and 850°C) and sintering time (1 and 2 hours). The polarisation method was conducted at 3 mV/s of a scan rate, and room temperature. According into the potentiodynamic polarization test, it was found that the sintering time of 2 hrs at constant temperature, and pressure enhances the corrosion potential towards stabilization the protective surface layer. A₃, A₄ are samples designation corresponding to different experimental settings determined by design of experiments. Corrosion current density measurements showed that A₄ sample had the highest (673.20 $\mu\text{A}/\text{cm}^2$), while A₃ sample had the lowest i_{corr} (0.8508 $\mu\text{A}/\text{cm}^2$). Tafel slope analysis revealed that A₃ sample had the highest anodic, and cathodic slopes, and was associated with the lowest corrosion rate. The corrosion resistance (R_p) data supported these results, with A₃ showing the highest resistance, confirming its superior corrosion resistance (R_p). This behaviour may be related into the noble properties of copper, and the protection of cupric oxide (CuO) compared to (NiO).

Keywords: Corrosion behavior, Functionally Grade Materials, Processing parameters, Potentiostat measurements, Corrosion parameters

1. Introduction

Friction, wear, corrosion and fatigue are common surface failures associated with engineering materials. The qualities of the material's surface directly affect how well the material performs. Surface coatings or deposits are utilised in many engineering applications to extend the life of components that are subjected to wear or corrosion. While the enhancement of the corrosion resistance of Cu-Ni alloys has received considerable attention, there is a dearth of research on the corrosion resistance of multi-layered Cu-Ni alloys. Functionally graded materials (FGMs) represent a significant advancement in materials science, characterized by a gradual variation in composition and properties

throughout the material [1, 2]. The materials of this group of presents a remarkable enhancement of previously used composite materials. FGM contains two or more materials whose combination permits certain characteristics achievement in accordance with the required application [3]. There are number of approaches to acquire the compositional gradient in the composite. This includes the solid phase, liquid phase and gas phase, which can be used to physically or chemically achieve tailored properties [4]. Advancements in manufacturing techniques like additive manufacturing and Chemical Vapor Deposition CVD have enabled the production of FGMs with complex geometries and tailored gradients that enhance performance under extreme conditions [5]. Functionally graded plasma-facing materials creation was explored using three distinct



processing techniques to produce W/Cu FGMs, SiC/C FGMs, and B₄C/Cu coated FGMs. The physical attributes, and microstructure of the FGMs are evaluated. The potential of these three FGMs as materials that interact with plasma in fusion reactors is demonstrated by certain plasma-relevant characteristics [6]. SiC/Cu FGM is a novel complex with exceptional mechanical properties since it effectively reduces interlayer thermal stress brought on by their mismatched thermal expansion coefficients at high heat flux. It combines the strong heat conductivity of copper and ductility with the benefits of silicon carbide, specifically its high melting point and strength. Consequently, it exhibits acceptable resistance to heat corrosion and thermal shock and could be used as a first-wall material in fusion reactors that face the plasma. The substantial melting point differential between silicon carbide and copper makes it exceptionally challenging to create this type of FGM using graded sintering method [7]. At Tokamak, graphite has been identified as a potential material for the International Thermonuclear Experimental Reactor (ITER) was determined to be a C/C composite. Nevertheless, C-based fabric displays an excessive chemical sputtering output at (326.85-726.85) °C and significantly increased sublimation at >926.85°C under plasma erosion conditions, resulting in the considerable C-contamination of plasma [8]. A new SiC/Cu functionally graded materials was created by using a cutting-edge technique known as graded sintering at extremely high pressure, which effectively formed a nearly dense graded composite [9]. The sinterability of W–Cu powders is mainly influenced by the particle size of the tungsten phase and the distribution of the copper phase. Composite particles, which consist of very fine tungsten grains embedded in copper, can be produced through high-energy milling [10, 11]. Real-time sintering observations in W/Cu system were achieved by exploiting the rearrangement densification technique using copper coated tungsten powders. Liquid Phase Sintering (LPS) is an effective processing technique for sintering the W–Cu system. As W and Cu are insoluble, densification via the solution precipitation process is inhibited. The only active methods of achieving density during LPS are rearrangement and solid-state sintering [12]. The Cu/W functionally graded materials were generated by vibrating W agglomerates to create a W skeleton with a porosity gradient, which was subsequently infiltrated with molten Cu after pressureless sintering. W/Cu FGMs may now be created in one step using a new technique termed resistance sintering under high pressure, without need for the sintering additives. A W/Cu FGM that was successfully produced has a theoretical density of more than 97% [13]. Helical Tokamak HT-7 was used for the fabrication and exposure of the plasma W/Cu FGMs with grain sizes of 0.2, 1, and 7 μm. This was achieved by the resistance sintering at extremely high pressure. Their mechanical characteristics and well-graded content distribution were discovered through microstructure analysis [14]. Materials for fusion power plants should have mechanical properties. In recent decades, numerous experiments have been conducted to quantify the changes in mechanical properties of irradiated steels and understand how radiation-induced damage forms. However, the lack of facilities makes it impossible to test potential materials in fusion-like environments. At this point, modelling is used to collect data and concepts that can be employed to estimate how damage to steel will affect its modifications [15]. Few works were conducted on

Cu-based alloys FGM [16] with no consideration for Cu–Ni alloys. In this work, the corrosion behaviour of Cu/Ni Functionally Graded Materials FGMs was investigated. FGMs were prepared using powder technology method with different compaction and sintering parameters. The effect of these factors on corrosion factors of corrosion potentials (E_{corr}), corrosion current densities (i_{corr}) and Tafel slope were examined.

2. Preparation of FGMs specimens

A cylindrical steel die with a diameter of (10 mm) was used to prepare the green FGMs compacts. The die surfaces were cleaned and lubricated with the liquid Paraffin. The predetermined mass of powder for each layer shown in Table 1 was carefully fed into the die starting from the 1st, 2nd, 3rd, 4th, and 5th layer. The powder for each layer was manually compacted to ensure the flatness of each layer, and then five layers were subjected to the pressing process through pressing machine.

Table 1.

Layers Composition, & mass

Layer No.	Weight (%)		Weight (gm)	
	Cu%	Ni%	Cu	Ni
1	100	0	7.91	0
2	75	25	1.1775	0.3925
3	50	50	0.785	0.785
4	25	75	0.3925	1.1775
5	0	100	0	3.15

Table 2 shows the variables adopted of applied pressure (P), sintering time (t), and sintering temperature (T), as well as their levels. A multi-level factorial design of experiments was conducted, and 18 experiments were examined. The samples resulting from the experiments are classified into three groups labeled A₁–A₆, B₁–B₆, and C₁–C₆ as shown in Table 3. The sintering practices were carried out by using vacuum furnace type (VDS/Ipsen, Germany) at the US Malaysia / School of Engineering.










Table 2.










Factors and their levels

Factors	Factor .1	Factor .2	Factor .3
Levels	T (°C)	t (hr)	P (MPa)
-1	650	1	0.7
0	750	2	1
+1	850	-	1.3

Table 3.

Full Factorial Design of Experiments

Experiment No.	Sample names	Factors			FGMs Samples
		$T (^{\circ}C)$	t (hr)	P (MPa)	
1	A ₁	-1	-1	-1	
2	A ₂	-1	0	-1	
3	A ₃	-1	-1	0	
4	A ₄	-1	0	0	
5	A ₅	-1	-1	+1	
6	A ₆	-1	0	+1	
7	B ₁	0	-1	-1	
8	B ₂	0	0	-1	
9	B ₃	0	-1	0	

10	B ₄	0	0	0	
11	B ₅	0	-1	+1	
12	B ₆	0	0	+1	
13	C ₁	+1	-1	-1	
14	C ₂	+1	0	-1	
15	C ₃	+1	-1	0	
16	C ₄	+1	0	0	
17	C ₅	+1	-1	+1	
18	C ₆	+1	0	+1	

3. Electrochemical Measurement

An electrochemical study was performed on a selection set of sintered FGMs samples (i.e. A₃, A₄, B₃, B₄, C₃, and C₄, as well as A₅, A₆, B₅, B₆, C₅, and C₆). Specimens with the cylindrical shapes were polished along its thickness, and acetone was used to degrease the specimens and rinse them with distilled water. The specimens were mounted by using formaldehyde at 138 °C for eight minutes to isolate sides except one, and to create a hole on one side for the electrical connection as shown in Figure 1.

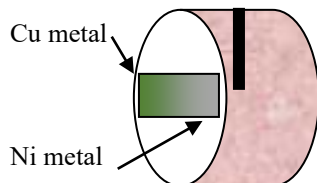


Fig. 1. Schematic of FGM mounted specimen

Potentiodynamic, and cyclic polarization measurements were performed using a Winking Mlab 200 Potentiostat (Bank-Electronic) with a standard electrochemical cell. Electrochemical measurements were performed using a potentiostat by SCI electrochemical software, and 3 mV/s scan rate. Polarization experiments were initiated with open circuit potential rate (EOCP) of less and more than (200mV).

The cathodic and anodic behaviour of FGMs shows distinct characteristics, at cathodic sites, oxygen reduction can occur to produce hydroxide ions as is shown in the following equation:



In the anodic region, metal oxidation occurs, which include Cu and Ni according to the nature of material as follow:



The key findings were presented in terms of corrosion potential (E_{corr}), corrosion current density (i_{corr}), and the measurement of Tafel slope by using method of the Tafel extrapolation.

4. Results and Discussion

Figure 2 illustrates the potential – time relationship, and Figure 3 shows potential-current density curves for a selection set of sintered FGMs samples (A₅, A₆, B₅, B₆, C₅ and C₆). The findings highlight that corrosion potentials take the following sequence:

$$-E_{\text{corr}} \quad \text{B}_5 > \text{B}_6 > \text{A}_5 > \text{C}_5 > \text{C}_6 > \text{A}_6$$

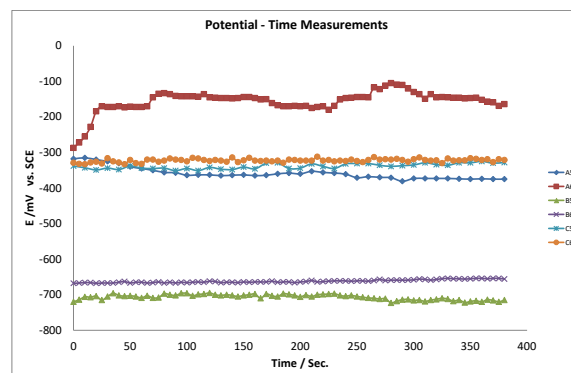


Fig. 2. Potential Vs time correlation

The figures display that these materials exhibit good resistance to local corrosion and there is no chance for pitting corrosion due to the presence of protective films in the structure of these materials and the disappearance of the hysteresis loop in cyclic behaviour in 3.5% NaCl solution. Ionic transfer of metal and oxygen occurs during both anodic and cathodic polarization. In a steady state, a notable example of this method is the passive anodic corrosion of metal. Such scenarios, migrate of the metal ions over the oxide layer at consistent rate, and participate in the reaction at oxide-electrolyte interface. The rate of dissolution of the passive layer is influenced by several factors, such as the local potential drop at interface, pH level and interaction between the ions of metal, and oxide surface. Anodic polarization refers to process where an electrode's potential is shifted in a positive direction due to current flow across the electrode-electrolyte interface. This shift results from electrochemical oxidation or anodic reactions near the anode surface, leading to a more noble potential for the anode [17]. Cathodic polarization, on the other hand, involves a shift in the electrode's potential in the negative direction, typically associated with reduction reactions. The formation and stability of passive oxide films on metal surfaces play a crucial role in protecting metals from corrosion. These films act as barriers that limit the transfer of ions and electrons, thereby reducing the metal's corrosion rate. The stability of these films is affected by environmental conditions like pH and the availability of specific ions in the electrolyte. Electrochemical techniques, including polarization measurements, are essential for understanding the corrosion behaviour of metals and alloys, especially those exhibiting active-passive behaviour. These techniques help in determining critical parameters like corrosion current density, corrosion potential and Tafel constants, which are vital to evaluate a material's resistance to corrosion [18].

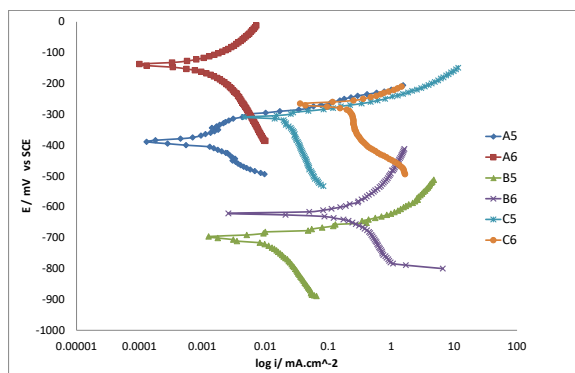


Fig. 3. Potential Vs current density correlation

The corrosion factors for corrosion potential (E_{corr}), corrosion current density (i_{corr}), polarization resistance (R_p), anodic, and cathodic Tafel slopes (b_a & b_c) of FGMs samples (A_3 , A_4 , B_3 , B_4 , C_3 and C_4) are shown in Table (4). Results obtained for the corrosion potential E_{corr} for specimen labelled A_4 , suggest that a corrosion potential of -138.6 mV, exhibits a nobler (more resistant to corrosion) compared to the material labelled A_3 , which has a corrosion potential of -388 mV. The data of E_{corr} show that B_4 sample exhibits a more noble with a potential (-617.6 mV) than B_3 sample which has a potential (-699.6 mV). It is observed that E_{corr} of C_4 sample (-265.2 mV) is more noble than C_3 sample (-310.8 mV). These results show that at a constant sintering temperature and compaction pressure, it was found that 2 hrs of sintering time for samples A_4 , B_4 , and C_4 gave a stable surface film at the material/ environment interface compared to 1hr sintering time for samples A_3 , B_3 , and C_3 . The measured data showed that the sample named A_3 has 0.8508 $\mu\text{A}/\text{cm}^2$ which is the lowest density of corrosion current, while, sample marked A_4 has 673.20 $\mu\text{A}/\text{cm}^2$ which is the highest current density. The corrosion current density (i_{corr}) is a kinetic factor, and represents the corrosion rate under specified equilibrium conditions. Any parameter that increases the value of (i_{corr}) results in an increase in value of the corrosion rate of the pure kinetic ground. Therefore, by comparing of the measured data, at constant sintering temperature and applied pressure, it was found that 2hrs of sintering time contributes to enhance corrosion current density of FGMs samples. Regarding Tafel slopes, samples C_3 and C_4 showed the lowest values, while A_3 sample demonstrated the highest value for the cathodic Tafel slope (b_c). In this context, sample B_3 showed the lowest value, and A_3 sample had the greatest value for the anodic Tafel slopes (b_a). This indicates that sample A_3 has the maximum values of the cathodic and anodic Tafel slopes respectively.

Table 4.

Corrosion parameters

FGM	$-E_{\text{corr}}$ (mV)	i_{corr} ($\mu\text{A}/\text{cm}^2$)	Tafel slope (mV/dec)		$R_p \times 10^3$ ($\Omega \cdot \text{cm}^2$)
			$-b_c$	$+b_a$	
A_3	388.4	0.8508	84.6	151.5	27.742
A_4	138.6	673.20	108.4	86.1	0.0310
B_3	699.6	11.530	250.0	33.5	1.1140
B_4	617.6	173.86	164.3	139.5	0.1887
C_3	310.8	20.500	362.8	38.8	0.7434
C_4	265.2	161.22	362.8	38.8	0.0945

It is detected that the current change rate with potential change was less significant during cathodic polarization than anodic polarization. A small cathodic slope shows a layer on surface of the tested material that is less permeable, and can hinder dissolution reaction of metal but allows an electrochemical reaction to occur. It is known that the surface oxide presents on the material allows ionic species and electrons or vacancies to flow through it [19, 20]. This result is an agreement with the result of corrosion current density that indicate that A_3 have lowest current density, i.e. lowest corrosion rate due to stable cupric oxide CuO . Polarization resistance (R_p) is similarly found from the Stern- Geary equation [21, 22].

$$R_p = \left(\frac{dE}{di} \right)_{i=0} = \frac{b_a * b_c}{2.303 * i_{\text{corr}} * (b_a + b_c)} \quad (4)$$

Values of R_p are shown in Table (4). These data indicate that the value of polarization resistance increases in the following sequence:

$$R_p \quad A_3 > B_3 > C_3 > B_4 > C_4 > A_4$$

This sequence is inversely consistent to the corrosion current density (corrosion rate) results, and confirms that sample A_3 has greater corrosion resistance compared to the other samples.

5. Conclusions

Copper/Nickel Functionally Graded Materials (FGMs) created through powder technology, with a composition gradient from 100% pure copper to nickel, demonstrate enhanced corrosion resistance due to the protective layers inherent in these materials. Corrosion resistance varies under various experimental conditions. Results of corrosion potentials, corrosion current density, and corrosion resistance of the tested samples indicate that a clear hierarchy of resistance, and sample A_6 the lowest while, sample B_5 exhibiting the highest. Specimen A_4 demonstrate more corrosion resistant than sample A_3 , and same trends were occurred with B and C series. Tafel slope analysis showed that sample A_3 had the lowest corrosion rate, confirmed by its high polarization resistance, and demonstrating superior corrosion resistance. A longer sintering duration significantly impact the corrosion behavior of these materials, increased corrosion current

density, and suggesting correlation between sintering time and corrosion rate.

Conflict of interest

The authors declare that they have no conflict of interest.

References

- [1] El-Galy, I.M., Saleh, B.I. & Ahmed, M.H. (2019). Functionally graded materials classifications and development trends from industrial point of view. *SN Applied Sciences*. 1, 1378, 1-23. <https://doi.org/10.1007/s42452-019-1413-4>.
- [2] Sahu, S. K., Chugh, R., Sahu, D., Khatri, R., Nagpal, S. & Shekhar, S. (2024). Innovations in functionally graded materials for advanced engineering applications. *Tuijin Jishu/Journal of Propulsion Technology*. 45(1), 2763 – 2775.
- [3] Mohammadi, M., Rajabi, M., & Ghadiri, M. (2021). Functionally graded materials (FGMs): A review of classifications, fabrication methods and their applications. *Processing and Application of Ceramics*. 15(4), 319-343. <https://doi.org/10.2298/PAC2104319M>.
- [4] Mahinzare, M., Ranjbarpur, H. & Ghadir, M. (2018). Free vibration analysis of a rotary smart two directional functionally graded piezoelectric material in axial symmetry circular nanoplate. *Mechanical Systems and Signal Processing*. 100, 188-207. <https://doi.org/10.1016/j.ymssp.2017.07.041>.
- [5] Alkunte S., Fidan I., Naikwadi V., Gudavasov S., Ali M.A., Mahmudov M., Hasanov S. & Cheepu M. (2024). Advancements and challenges in additively manufactured functionally graded materials: a comprehensive review. *Journal of Manufacturing and Materials Processing*. 8(1), 23- 1-37. <https://doi.org/10.3390/jmmp8010023>.
- [6] Ge, C-C., Li, J-T., Zhou, Z-J., Cao, W-B., Shen, W-P., Wang, M-X., Zhang, N-M., Liu, X. & Xu, Z-Y. (2000). Development of functionally graded plasma-facing materials. *Journal of Nuclear Materials*. 283-287(2), 1116-1120. [https://doi.org/10.1016/S0022-3115\(00\)00318-4](https://doi.org/10.1016/S0022-3115(00)00318-4).
- [7] Ling, Y., Ge, C., Li, J. & Huo, C. (2000). Fabrication of SiC/Cu functionally gradient material by graded sintering. *Functionally graded materials 2000*. 114, 333-340.
- [8] Ge C.C., Wu A.H., Ling Y.H., Cao W.B., Li J.T. & Shen W.P. (2002). New progress of ceramic-based functionally graded plasma-facing materials in China. *Key Engineering Materials*. 224-226, 459-464. <https://doi.org/10.4028/www.scientific.net/KEM.224-226.459>.
- [9] Ling, Y-H., Li, J-T., Ge, C-C. & Bai, X-D. (2002). Fabrication and evaluation of SiC/Cu functionally graded material used for plasma facing components in a fusion reactor. *Journal of Nuclear Materials*. 303(2-3), 188-195. [https://doi.org/10.1016/S0022-3115\(02\)00801-2](https://doi.org/10.1016/S0022-3115(02)00801-2).
- [10] da Costa, F. A., da Silva, A. G. P., & Gomes, U. U. (2003). The influence of the dispersion technique on the characteristics of the W–Cu powders and on the sintering behavior. *Powder Technology*. 134(1-2), 123-132. [https://doi.org/10.1016/S0032-5910\(03\)00123-2](https://doi.org/10.1016/S0032-5910(03)00123-2).
- [11] Ozkal, B., Upadhyaya, A., Ovecoglu, M. L. & German, R. M. (2004). Realtime sintering observations in W-Cu system: accelerated rearrangement densification via copper coated tungsten powders approach. *Euro PM Sintering*. 1-7.
- [12] Jankovic' Ilic, D., Fiscina, J., Gonzalez-Oliver, C.J.R. & Mucklich, F. (2005). Properties of Cu-W functionally graded materials produced by segregation and infiltration. In *Functionally Graded Materials*, proceedings of the 8th international symposium on multifunctional and functional graded materials. Materials Science Forum, Vol. 492-493, (pp. 123-128). Belgium.
- [13] Zhou, Z. J., Du, J., Song, S. X., Zhong, Z. H., & Ge, C. C. (2007). Microstructural characterization of W/Cu functionally graded materials produced by a one-step resistance sintering method. *Journal of Alloys and Compounds*. 428(1-2), 146-150. <https://doi.org/10.1016/j.jallcom.2006.03.073>.
- [14] Chong, F.L., Chen, J.L., Zhou, Z.J. & Li, J.G. (2008). Fabrication and plasma exposure of fine-grained tungsten / copper functionally graded materials in the HT-7 tokamak. *Fusion Science and Technology*. 53(3), 854-859, <https://doi.org/10.13182/FST08-A1740>.
- [15] Stephane Alexis Jacques Forsik, (2009). *Mechanical properties of materials for fusion power plants*. Ph.D. Thesis, Darwin College, Cambridge, Germany.
- [16] Güler, O., Varol, T., Alver, Ü. & Biyik, S. (2021). The wear and arc erosion behavior of novel copper based functionally graded electrical contact materials fabricated by hot pressing assisted electroless plating. *Advanced Powder Technology*. 32(8), 2873-2890. <https://doi.org/10.1016/j.apt.2021.05.053>.
- [17] Sohail, M.G., Laurens, S., Deby, F., Balayssac, J.P. & Nuaimi, N.A. (2021). Electrochemical corrosion parameters for active and passive reinforcing steel in carbonated and sound concrete. *Materials and Corrosion*. 72(12), 1854-1871. <https://doi.org/10.1002/maco.202112569>.
- [18] Schultze, J.W. & Lohrengel, M.M. (2000). Stability, reactivity and breakdown of passive films. Problems of recent and future research. *Electrochimica Acta*. 45(15-16), 2499-2513. [https://doi.org/10.1016/S0013-4686\(00\)00347-9](https://doi.org/10.1016/S0013-4686(00)00347-9).
- [19] Traldi, S.M., Rossi, J.L. & Costa, I. (2001). Corrosion of spray formed Al-Si-Cu alloys in ethanol automobile fuel. *Key Engineering Materials*. 189-191, 352-357. <https://doi.org/10.4028/www.scientific.net/KEM.189-191.352>.
- [20] Traldi, S.M, Rossi, J.L. & Costa, I. (2003). An electrochemical investigation of the corrosion behavior of Al-Si-Cu hypereutectic alloys in alcoholic environments. *Revista de Metalurgia Suplementos*. 86-90.
- [21] Stern, M. (1958). Method for determining corrosion rates from linear polarization data. *Corrosion*. 14(9), 60-64. <https://doi.org/10.5006/0010-9312-14.9.60>.
- [22] Stern, M. & Geary, A.L. (1957). Electrochemical Polarization I: A Theoretical Analysis of the Slope of Polarization Curves. *Journal of the Electrochemical Society*. 104(1), 59-63. DOI: 10.1149/1.2428496.